11. Damage of Optical Elements

Optically induced damage to the laser medium and to components of the laser system generally determine the limit of useful performance of solid-state lasers. The performance of a laser system in terms of pump efficiency, gain, nonlinear conversion, brightness, and beam quality increases with power density of the beam. Power density is fairly independent of the size of the laser, output power scales mostly with beam diameter rather than beam intensity. As a consequence, it is desirable to operate all lasers at the highest beam intensity consistent with reliable operation, which, in turn, is determined by the optical-damage threshold of the various components. Therefore, an understanding of the mechanisms which cause radiation damage to optical components and a knowledge of the damage threshold of the materials employed in a laser are of great importance to the engineer who is designing a laser system.

Damage may occur either internally or at the surface of an optical component owing to a number of intrinsic and extrinsic factors. Intrinsic processes that limit the optical strength of materials include linear absorption, color-center formation, and a variety of nonlinear processes such as self-focusing, multiphoton absorption, and electron avalanche breakdown. Extrinsic factors include impurities, material defects (voids, dislocations, etc.), and in particular surface scratches and digs and surface contamination. In general, damage threshold is determined by the condition of the optical surfaces and the quality of optical coatings rather than by the bulk material. The problem of surface damage is compounded because most laser systems contain many surfaces.

There are different ways of defining damage threshold. One might define damage as the physical appearance of a defect in the material or by a degradation in the output performance of the laser system. From the standpoint of the user of the laser system, the performance deterioration is of more importance than the physical appearance of a defect in the material. Often the occurrence of a small blemish or defect does not alter system performance. In this case it is important to determine whether the defect remains constant or increases with time.

Quantitative measurements of the damage threshold of an optical component should be performed following a procedure specified by the International Standards Organization [11.1–3]. A test sample is irradiated with a well-characterized laser at different sites. The fluence levels are chosen so that at the higher fluence a high probability of damage exists, whereas at the lower levels the probability of damage is low. The percentage of failures is plotted vs. fluence. A least-squares linear fit to this data is calculated.

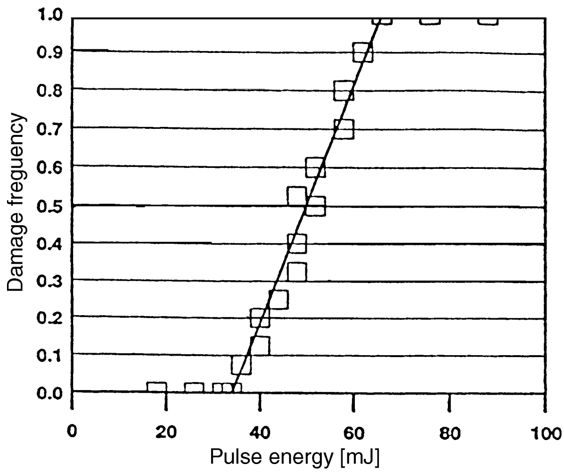

Fig. 11.1. Damage frequency plot for defining 0% damage probability according to ISO 11254

The linear data extrapolation to 0% damage frequency is defined as the damage threshold. The testing sites are inspected for damage with a Nomarski microscope at a magnification of 150. Figure 11.1 shows a damage frequency plot according to ISO 11254.

The results of experimental and theoretical investigations of laser-induced damage in dielectric and sol-gel coatings, optical glasses, metal films, laser crystals and glasses, crystals used in polarizers, Q-switches, harmonic generators, and parametric oscillators are presented annually at the Boulder Damage Symposium held since 1969. The earlier proceedings of these symposia have been published by the National Bureau of Standards [11.4] and since 1990 by the International Society for Optical Engineering (SPIE) [11.5]. Selected papers from the earlier symposia have also been published in a book [11.6].

11.1 Surface Damage

Undoubtedly the weakest parts in a well-designed laser are the surfaces of the optical components. It has been found that surfaces, even those that are scrupulously cleaned, have a lower damage threshold than the bulk.

One reason for the lower surface-damage threshold compared to bulk damage stems from the fact that even after the polishing process used in the finishing of optical elements, there are residual scratches, defects, and imperfections on the surface. At these points, the electric field of the light wave is greatly intensified so that the effective field value just inside the surface is much greater than the average field. When breakdown or failure of the surface occurs, it occurs near one of these imperfections [11.7]. Furthermore, as a consequence of the polishing process, minute inclusions of polishing material or other impurities are embedded in the surface. These impurities may be strongly absorbing and, if so, can provide a nucleus around which damage may occur. Other factors tending to lower the damage threshold at the surface are contamination of the surface due to airborne particles, fingerprints, and residue from outgassing of nearby components.

From the foregoing it follows that surface damage is caused either by absorption of submicrometer inclusions or by the formation of a plasma at the surface because of electron avalanche breakdown in the dielectric materials. In the former case, microexplosions of isolated inclusions occur just under the surface [11.8]. In the latter case, the electric field produced by an intense laser beam is so high that the dielectric material will break down [11.9].

This avalanche ionization represents the ultimate failure mode of dielectric materials. In this process, a few free charge carriers from easily ionized impurities, or as a result of multiphoton ionization, absorb energy from the oscillating electric field of the light wave. Hence, they gain kinetic energy and multiply by impact ionization of the solid-state lattice. As a result of avalanching, the concentration of electrons increases significantly, which leads eventually to a complete absorption of radiation. The avalanche breakdown is usually associated with a luminous plasma formed in the material. The avalanche process is the high-frequency analog of dc breakdown. Avalanche ionization is the primary cause of surface damage, once absorbing impurities are removed. Because of field intensification effects, avalanche ionization is more likely to occur in the vicinity of pits and scratches at the surface.

The reduction of damage threshold at imperfect surfaces owing to multiple reflections has been analyzed in [11.7]. It was found that depending on the defect geometry, the presence of surface pits, grooves, cracks, nodules, or voids can increase the local field intensity by a factor up to n^4, where n is the refractive index.

More recently it was reported that interference of internal reflections at a crack and the surface can locally cause much higher radiation intensification [11.10]. The numerical calculations revealed that light intensity enhancements are very sensitive to the polarization and angle of incidence of the beam, and the orientation and width of a crack with respect to the surface. For conical cracks the light intensity enhancement factor can locally reach two orders of magnitude.

In some cases a dielectric coating applied to a surface raises the damage threshold. Micropits and scratches are filled in by the coating material, which then reduces the reflectivity and standing wave ratio in association with smoothing of the surface. This effect has been observed in such cases as MgF_2 on glass, ThF_4 on $LiNbO_3$, and sol-gel AR coatings on fused silica.

Super-polishing techniques, such as ion polishing and chemical etching, lead to higher damage thresholds than those for conventionally polished optical surfaces. Superpolish produces surfaces with a rms roughness of less than 1 Å, whereas a normal high-quality polish has a surface roughness of 10–20 Å.

Surface damage typically takes the form of a pit and is observed more frequently at the exit surface rather than the entrance surface of an optical component. Several models have been proposed to explain these observations.

In one model, pit formation and the difference of damage between front and back surface have been explained to be the results of reflections occurring at the various boundaries [11.11, 12]. The formation of pits in glass is assumed to be the result of a standing wave which is formed inside the glass near the surface. The standing wave is caused by reflections from the plasma-glass boundary. After plasma initiation there is a layer of plasma several wavelengths thick contiguous to the surface. This plasma is densest at its source, that is, next to the surface. The electric field at the antinodes of this standing wave can become twice as large as the electric field of the incident beam. The first antinode is within one-quarter wavelength of the surface. It is this large electric field at the antinode that initiates pitting at, or just inside, the surface.

The fact that a sample of transparent dielectric material exposed to a collimated beam of light will usually damage at the exit surface at a lower power level than at the entrance surface can also be explained by the effect of Fresnel reflection. When a light pulse enters an isotropic optical material at near-normal incidence, there is a reflection at the air-to-sample boundary. Since the index of refraction n of the material is higher than that of air, the reflected light wave suffers a phase shift of 180° with respect to the incident light wave. This phase shift results in a partially destructive interference of the two light waves within a distance of $\lambda/4$ of the entrance surface. As a result the light intensity I_{en} at the entrance surface is related to the incident intensity I_0 by

$$I_{en} = \frac{4}{(n+1)^2} I_0. \tag{11.1}$$

At the exit surface, the reflected wave suffers no phase shift, so that the intensity at the exit surface I_{ex} is related to the intensity incident on the sample by

$$I_{ex} = \left(\frac{4n}{(n+1)^2} \right)^2 I_0. \tag{11.2}$$

Thus the ratio of the intensity inside the medium at the exit surface to the intensity inside the medium at the entrance surface is

$$\frac{I_{ex}}{I_{en}} = \left(\frac{2n}{n+1} \right)^2. \tag{11.3}$$

For $n = 1.55$, this ratio is 1.48.

A model which explains another difference between contaminated entrance and exit surfaces was put forward in [11.13]. However, the same conclusion is reached, namely, that particles on the front surface cause less damage than on the back surface. On the exit surface, a plasma is formed and confined between two solid materials, i.e., the substrate and the particle. The high density of the plasma and associated pressure cause the particle to be ejected rapidly on heating. The reaction force leads to a small pit on the surface, which then leads to damage. On the front surface, the plasma can expand and only a weak shockwave is launched into the substrate, and the surface is not pitted or damaged. Small particles may be completely vaporized in the process.

Consistent with the particle ejection model is the observation that internal reflective surfaces of Porro prisms and corner cubes have generally a higher damage threshold if the reflective surfaces are coated with SiO_2 coatings of about 2 μm thickness. The coating prevents the field of the evanescent wave from reaching the particles and therefore prevents the initiation of reaction pits.

11.2 Inclusion Damage

Optical components tend to exhibit minute inhomogeneities, which generally form in the process of fabricating the material. The inhomogeneities can consist of small bubbles, dielectric inclusions, or platinum particles in the case of laser glass. In crystalline materials, although some microinhomogeneities do occur during the growth process, there is less evidence that particulate damage is the limiting factor. In glass, however, during the course of melting, crucible material finds its way into the melt and upon cooling condenses out in the form of particulate inclusions. This has been a particularly difficult problem in the fabrication of laser glass, which is manufactured in platinum containers. The problem of platinum inclusions has been solved by glass manufacturers either by using crucibles of ceramic and clay materials or by carefully controlling the oxygen content in the melt. If the material contains minute inhomogeneities such as particulate inclusions, especially metallic inclusions, they can absorb the laser radiation, giving rise to local heating and melting of the surrounding laser host material. This in turn causes stress concentrations sufficient to rupture the material. Elaborate theoretical treatments of the problem of stress formation in the vicinity of an absorbing particle have been published [11.14].

To summarize the considerations that apply, let us consider an absorbing particle embedded in a laser material, illuminated by a brief and intense pulse of light. If the particle is a sphere of diameter d, it presents an absorbing area to the incident light of $\pi d^2/4$. The total energy absorbed in the particle is approximately

$$\Delta E = I t_{\mathrm{p}} \left(\frac{\pi d^2}{4} \right) (1 - e^{-\alpha d}), \tag{11.4}$$

where I is the power density, t_{p} is the pulse duration, and α is the material absorption coefficient. The maximum temperature rise experienced by the particle will be given by

$$\Delta T = \frac{\Delta E}{C_{\mathrm{p}}(\pi d^3/6)\gamma}, \tag{11.5}$$

neglecting heat conduction during the pulse. In the above equation C_{p} is the specific heat and γ is the density of the inclusion.

Equation (11.5) indicates that the temperature of metal particles subject to a 20-J/cm^2, 30-ns laser pulse can exceed 10,000 K for typical particle sizes. These high temperatures produce stress in the glass adjacent to the particles, which can exceed the theoretical strength of glass and result in failure.

11.3 Damage Threshold of Optical Materials

The data presented here on bulk, surface, and dielectric thin-film damage levels should only be used as a guide, since damage thresholds depend on a great number of laser and materials parameters, as well as sample cleanliness and prior history. Laser parameters, such as wavelength, energy, pulse duration, transverse and longitudinal mode structure, beam size, location of beam waist, all play an important part in the definition of damage threshold. For example, multimode beams usually contain "hot spots" at which the peak power is many times the average value estimated from the pulse energy, pulse duration, and beam cross section.

Experience also shows that the damage threshold can vary greatly even within one particular sample because of compositional variations, localized imperfections, absorption centers, etc. It has also been shown that the prior history of a sample can have a large influence on the damage level.

11.3.1 Scaling Laws

Although the specific threshold at which laser damage is observed depends on a great many factors, empirical scaling laws offer a guide to the parametric variation of the thresholds for a given material.

In this subsection, the dependence of damage threshold on pulse width, wavelength, beam diameter, and laser conditioning is discussed.

Pulse Width. We can distinguish two different behavioral regimes. For pulses longer than about 100 ps, damage is caused by conventional heat deposition resulting in melting and boiling [11.15, 16]. Energy is absorbed by conduction band electrons from the external field and transferred to the lattice. In this regime, the source of the initial seed electrons can be local defects or impurities. For damage to occur, the temperature near the local absorption centers must be sufficiently high to cause fracture or melting.

Because the limiting process for temperature growth is thermal conduction and diffusion into the lattice, the fluence required to raise the heated region to some critical temperature is proportional to $t_p^{0.5}$ where t_p is the pulse duration [11.17]. This is in reasonably good agreement with numerous experiments which have observed a t_p^{α} scaling with α between 0.3 and 0.6 in a variety of dielectric materials from 20 ps to over 100 ns, including samples with defects.

Figure 11.2 illustrates the dependence of damage threshold on pulse width for a number of materials. The data presented are the results of numerous measurements performed at the Lawrence Livermore National Laboratory over a period of 10 years [11.18]. The materials include silicate glasses, such as borosilicate BK-7, low-expansion TiO_2–SiO_2 (ULE), fused silica, a commercial phosphate glass (LG 750), fluorophosphate glass, a sol-gel AR coating and a high reflectivity dielectric coating HfO_2 on a fused silica substrate.

The pulse-width dependence ranges from $t_p^{0.5}$ for fused silica at 355 nm and the sol-gel AR coating to $t_p^{0.4}$ for fused silica, BK-7, ULE, LG 750, and fluorosphosphate at 1064 nm, and to $t_p^{0.3}$ for the HfO_2 coating.

As the pulse width decreases below 100 ps, a gradual transition takes place from the long pulse, thermally dominated regime to an ablative regime dominated by collisional and multiphoton ionization and plasma formation [11.19–21]. For pulses shorter than

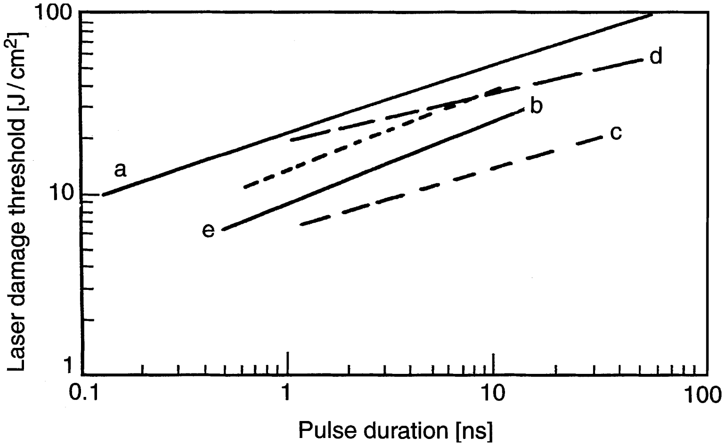

Fig. 11.2. Damage threshold vs. pulse duration for fused silica, BK-7, ULE, LG 750, and flurophosphate glass at 1064 nm (a); fused silica at 355 nm (b); HfO_2/SiO_2 HR coating at 1064 nm, unconditioned (c) and laser conditioned (d); sol-gel AR coating on fused silica at 1064 nm and 355 nm (e) [11.18]

about 20 ps, electrons have insufficient time to couple to the lattice during the laser pulse. The damage threshold continues to decrease with decreasing pulse width, but at a rate slower than $t_p^{0.5}$. This departure is accompanied by a qualitative change in the damage morphology indicative of rapid plasma formation and surface ablation. The damage site is limited to only a small region where the laser intensity is sufficient to produce a plasma with essentially no collateral damage.

Optical breakdown occurs because of an electron avalanche in which conduction-band electrons, oscillating in response to the laser field, achieve energy equal to the bandgap, and subsequent impact ionization promotes another valence electron into the conduction band. Because the pulses are so short, collisional heating of the electrons occurs before there is significant transfer of energy from the electrons to the lattice. Impact ionization eventually results in an electron avalanche [11.9, 22].

Wavelength Dependence. Typically, the damage threshold decreases for shorter wavelengths and drops off rather sharply at the shortest wavelengths. This behavior is illustrated in Fig. 11.3 which summarizes the results of over 1000 damage measurements on KDP crystals [11.23]. The sharp drop in bulk damage threshold for very short wavelengths has also been measured in fused quartz and synthetic fused silica [11.24]. Fused quartz is produced by melting natural quartz powder, and synthetic fused silica is produced directly by flame hydrolysis of $SiCl_4$ in an H_2/O_2 flame. Measurements were performed with a Q-switched laser at 1064, 532, 355, and 266 nm with pulses of about 1 ns. For silica glass the laser-induced bulk damage threshold can be expressed as

$$J_{th} = 1.45\lambda^{0.43}, \tag{11.6}$$

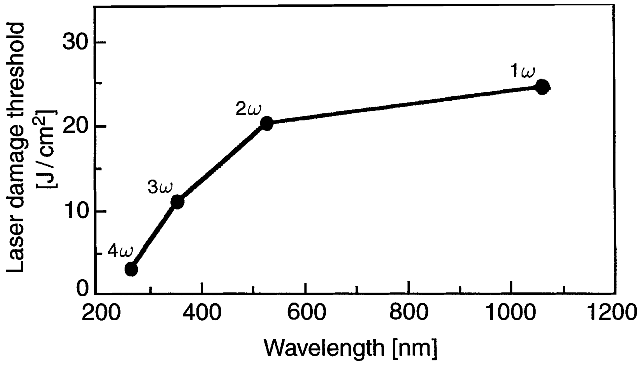

Fig. 11.3. Bulk laser damage threshold of KDP crystals measured with 3-ns pulses at the fundamental and harmonics of an Nd:YAG laser [11.23]

where J_{th} is in J/cm^2 and λ is the wavelength in nm. This relationship holds for wavelengths between 1064 and 355 nm. At 266 nm the threshold is about a factor 2 lower than that calculated from the above equation. It was concluded that the damage mechanism at wavelengths shorter than 355 nm is determined by two photon absorption. At 1064 nm no difference was found between the various types of SiO_2; at shorter wavelengths fused quartz samples had a slightly smaller damage threshold compared to synthetic fused silica.

Other experimental data for bulk and sol-gel AR-coated fused silica show a similar decrease in damage threshold in changing the wavelength from 1064 to 355 nm [11.18, 25].

Spot-Size Dependence. Surface damage is usually initiated by defects, such as pits, inclusions, or scratches. Probing the surface with a beam smaller than the separation of isolated defects will measure the damage threshold of the basic substrate or coating material. A larger spot size will increase the probability that surface defects will be within the beam area. Therefore, there is a dimensional dependence of the damage threshold. Depending on the density and distribution of these imperfections at a certain spot size, the dimensional dependence will disappear.

The dimensional dependence indicates that the failure mechanism is due to defect-driven localized failures rather than the basic coating or substrate material. In testing for damage, it is important that the beam spot size is large enough to provide meaningful results. Figure 11.4 illustrates a typical result of a dielectric coating tested at different spot diameters [11.26]. The dimensional dependence of the damage threshold disappears for spot sizes larger than 100 μm.

Laser Conditioning. It has been consistently observed in a number of optical materials, both bulk and thin film, that the damage threshold can be substantially and permanently improved by a process which consists of exposing a component to

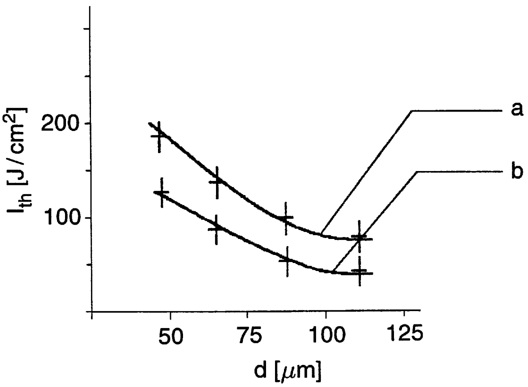

Fig. 11.4. Damage threshold dependence on beam diameter of a ZrO_2/SiO_2 (*curve a*) TiO_2/SiO_2 (*curve b*) multilayer coating [11.26]

incrementally higher and higher fluence levels beginning well below the single-shot damage threshold [11.27–30].

Multilayer HfO_2 coatings on fused silica substrates show the most consistent improvement with laser conditioning. In general, conditioning produces about a two to threefold improvement in the damage threshold. The curves (c and d) in Fig. 11.2 illustrate this improvement. The conditioning effect has been associated with the gentle removal of nodular-shaped defects, which are known to limit the damage threshold of these multilayer coatings. Other dielectric coatings which have been reported to respond to laser conditioning are MgF_2, LaF_3, and ZrO_2 [11.31, 32]. The bulk damage of KDP crystals can also be increased by a factor of 2 or more over the unconditioned threshold [11.23].

Actually, laser conditioning may represent the greatest single practical improvement in thin-film damage thresholds in the past 10 years. As a general rule of thumb at least five shots are needed to condition the optic to $\approx$85% of the maximum conditioned threshold. Furthermore, the first shot in the conditioning sequence should be at a fluence of about one-half the unconditioned damage threshold.

11.3.2 Laser Host Materials

The damage threshold of the laser medium is usually determined by the coatings rather than the bulk material. Internal damage occurs relatively seldom, unless an internal focus is created because of self-focusing, or as a result of back reflections from an optical element.

Bulk damage using 47-ps pulses from a mode-locked Nd:YAG laser at 1.06 μm has been measured for a number of materials by focusing the beam inside the sample [11.33]. The samples tested included LiSAF, LiCAF, and LiSCAF, with different chromium dopings, along with Nd:YAG, fused silica, and BK-7. The threshold value of the Cr-doped laser crystals was about 20 J/cm^2 or 400 GW/cm^2, which are comparable with those of fused silica and BK-7 and about a factor of 2 larger than Nd:YAG.

Bulk damage threshold measurements with a Q-switched Nd:YAG laser which had a pulse width of 10 ns are reported in [11.34]. The lowest power density for which damage was observed in the Nd:YAG sample was 3.6 GW/cm^2, and 2.6 GW/cm^2 for Nd:YALO. As a comparison, the intrinsic damage thresholds for $LiNbO_3$ and calcite were at least a factor 6 lower compared to the laser crystals. Bulk damage thresholds for a number of Nd:Glasses have already been summarized in the previous section.

Although this chapter is concerned with laser-induced damage to optical materials, it might be of interest to some readers to briefly mention damage to laser crystals induced by gamma and proton radiation. Solid-state lasers in space are exposed to charged particles, such as electrons, protons, and high-energy cosmic rays. The effect of gamma rays and high-energy protons on Nd:YAG and Nd:YLF crystals has been described in [11.35]. It was found that both forms of radiation create color centers in the crystals which reduced optical output primarily by absorbing the laser radiation.

For Nd:YAG the induced absorption loss reached a limiting value of about 0.015 cm^{-1} at 100 krad exposure levels; the loss in Nd:YLF was higher and did not reach a limiting value. Codoping Nd with Cr^{3+} significantly reduced radiation susceptibility of Nd:YAG. The result of the experiments suggested that diode-pumped Nd:YAG lasers can be effectively radiation-hardened to withstand exposure to charged particles in space. Design features which improve radiation hardness include codoping of the Nd:YAG crystal with Cr^{3+}, a short laser crystal, and pulsed Q-switched rather than cw operation, because the higher gain can more readily overcome the induced losses created by color centers.

11.3.3 Optical Glass

Data on bulk damage thresholds for a number of glasses have been provided in Sect. 11.3.1. In inclusion-free silica, damage threshold is limited by the surface. Extensive measurements at different wavelengths and pulse widths give a simple empirical relationship governing the safe operating limit for fused silica [11.25]

$$J_{\mathrm{th}} = (22 - 25)t_{\mathrm{p}}^{0.4} \quad \text{at } 1064\,\mathrm{nm},$$
$$J_{\mathrm{th}} = (9 - 14)t_{\mathrm{p}}^{0.5} \quad \text{at } 355\,\mathrm{nm}.$$

The lower values are for bare surface fused silica, and the higher values are measured after a sol-gel AR coating is applied to the surface. J_{th} is the damage threshold (J/cm^2) and t_{p} is the pulse length (ns). In agreement with the common trend in optical materials, the measurements also reveal a substantial decrease of the damage threshold for the shorter wavelength.

For pulses shorter than 20 ps, the damage fluence no longer follows the $t_{\mathrm{p}}^{0.5}$ dependence. As explained earlier, for such short pulses there is insufficient time for lattice coupling. Figure 11.5 summarizes measurements of the damage fluence for fused silica at very short pulse widths [11.21]. Summaries of the damage threshold of a large number of different optical glasses including absorption filters can be found in [11.36].

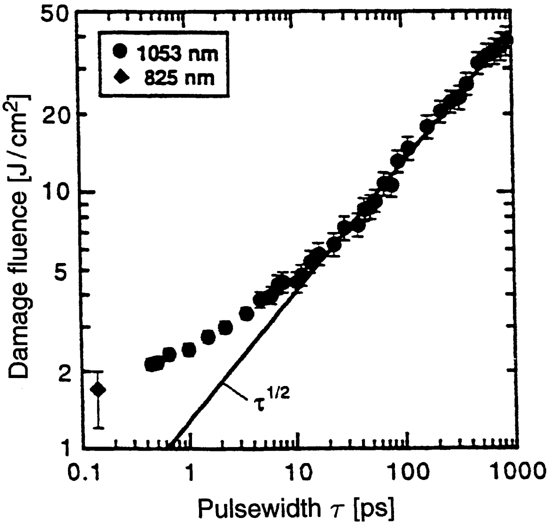

Fig. 11.5. Threshold damage fluence for fused silica as a function of pulse width [11.21]

11.3.4 Nonlinear Crystals

From all the optical components and materials employed in solid-state laser systems the largest spread in damage thresholds occurs with nonlinear crystals. Table 11.1 summarizes the nominal damage levels of important crystals employed in nonlinear process of solid-state lasers. It shows a spread of over two orders of magnitude from KDP/KD*P to the $AsGaSe_2$/$AsGaS_2$ crystals.

In addition to exhibiting damage mechanisms operative in other dielectric materials, such as thermal heating, and creation of an electron avalanche by impact ionization, nonlinear materials are subject to damage by virtue of their nonlinear properties. It is frequently observed that the damage levels observed in harmonic generation are far lower in the presence of the harmonic than those observed with just the fundamental present. This effect is often caused by multiphoton absorption, which plays a major role in laser-induced damage in nonlinear crystals. In this process, 2-photons or 3-photons can generate radiation at a wavelength which is below the absorption edge of the crystal. Absorption of UV radiation typically leads to color center formation.

Table 11.1. Typical damage thresholds for nonlinear crystals

Nonlinear crystal	KDP	KD*P	LBO	BBO	KTP KTA	$LiNbO_3$ PPLN	$AsGaS_2$ AsGaSe
Damage threshold [GW/cm^2]	8	4	2.5	1.5	0.5	0.2	0.03

Laser-induced damage in KDP and KD*P has been studied in great detail because these crystals are employed in inertial confinement fusion lasers for the generation of the second and third harmonics from Nd:Glass lasers. Laser damage threshold for KDP as a function of wavelength is depicted in Fig. 11.3. The damage threshold for KD*P is about a factor 2 lower compared to KDP. As already mentioned the threshold for bulk damage can be increased by subjecting the crystals to a series of gradually increasing fluence levels beginning below unconditioned threshold levels [11.37, 38].

The borate crystals LBO and BBO also have very high damage thresholds. LBO is emerging as an alternative to KTP for harmonic generation of Nd:lasers. This crystal does not suffer from nonlinear absorption or photo-refractive effects; however, the nonlinear coefficient and thermal acceptance parameter of LBO are about one third those of KTP. Lifetimes in excess of 1000 hours have been reported in LBO at a second-harmonic output close to 180 W [11.39]. BBO has a transmission band which extends to 200 nm; therefore, multiphoton absorption is not a problem. This material is of particular interest for harmonic generation in the blue region of the spectrum.

KTP crystals are primarily employed for frequency doubling of Nd:lasers, and in OPOs for the generation of the eye-safe wavelength of 1.5 μm. Although the bulk and surface damage thresholds for KTP are quite high at 1.06 μm, employed in a second harmonic generator or as an OPO, a number of failure mechanisms set in which are related to the conversion process.

At around 1.06 μm, laser-induced damage in KTP is associated with surface coatings and macroscopic flaws in crystals. The damage threshold of KTP at 1.06 μm, measured with a Q-switched Nd:YAG laser with a pulse width of 20 ns, is depicted in Fig. 11.6.

Nonlinear effects were minimized in these tests by appropriate orientation of the crystal. Surface failure for uncoated crystals is typically 15–20 J/cm^2 for pulse width

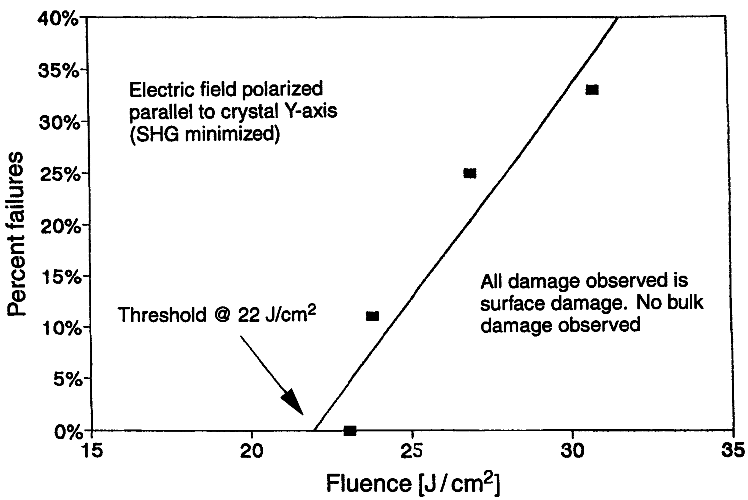

Fig. 11.6. Damage frequency plot of KTP at 1064 nm [11.40]

of 10–20 ns. Bulk failure thresholds have been measured as high as 30 GW/cm^2 [11.40, 41].

When KTP is used in a noncritical phase-matched OPO, it is subject to thermal heating owing to 3.3-μm idler absorption. In high-average-power systems this absorption results in a substantial lowering of the damage threshold. With a 20 Hz Nd:YAG laser, massive bulk and surface damage was observed at fluence levels as low as 5 J/cm^2 [11.40, 41].

KTA, a crystal very similar to KTP, has much lower absorption at the idler wavelength (Fig. 10.12). KTA avoids the problems associated with thermal heating due to absorption in the 2.8–3.5 μm region. Consequently KTA, rather than KTP, is usually employed in high-average-power OPOs designed for the generation of infrared radiation from an Nd:laser.

Damage of KTP in a harmonic generator results from a photochromic process which forms laser-induced color centers commonly referred to as gray tracks. Absorption of both the fundamental and harmonic radiation along the beam volume leads eventually to catastrophic failure of the crystal.

Different crystalline defects such as the presence of Ti^{3+} or Fe^{3+} chemical impurities, or a stoichiometric imbalance creating oxygen vacancies, can lead to different damage mechanisms [11.42]. The cause of damage is generally believed to be a nonlinear photoionization process such as multiphoton absorption, third harmonic, or sum frequency generation. These processes can produce photons with energies greater than the bandgap energy of KTP. These energetic photons will create free electrons and holes, some of which will become trapped at defect sites in the crystal. These defects may initially be nonabsorbing, but when ionized they become strongly absorbing. Active hole traps are Fe^{3+} impurities and active electron traps are Ti^{4+} ions which are adjacent to an oxygen vacancy [11.43]. Another damage mechanism leading to gray tracks at 532 nm is two-photon absorption by Ti^{3+} color centers [11.44].

Gray tracking in KTP has been extensively investigated [11.42–53]. Gray-tracking damage can be removed by heating the crystal during operation to about 70–100°C. At this elevated temperature darkening due to the photochromic process is annealed out fast enough to achieve long-term stable operation. Higher temperatures will accelerate the annealing process even more.

Gray tracking decreases as the temperature increases and vanishes for temperatures above 170°C [11.44]. In a laser system a higher temperature has to be weighted against potential contamination problems from outgassing of the hot components of the crystal oven (Sect. 11.4).

In a test conducted at 75°C, exposure to 12 J/cm^2 and 10,000 shots produced no bulk darkening; the same experiment performed at 30°C caused a transmission loss ranging from 4 to 8% [11.47].

Intracavity-doubled Nd:YAG lasers have produced over 100 W of second-harmonic power using KTP. In one of these high-power systems a degradation rate was measured of 0.04% per hour during a 300-h test run at 150 W of green output and a repetition rate of 13 kHz. Most of the degradation was attributed to gray tracking in the KTP crystal [11.39]. Because of this high degradation rate, the KTP crystal was replaced by an LBO crystal. Degradation of LBO operated at 30°C was negligible at an average green output of 180 W.

In our laboratory, we have built a number of diode-pumped Nd:YAG lasers which produce between 250 and 500 mJ per pulse of green output at a pulse width of 10–20 ns and repetition rates up to 100 Hz. At a fluence level of about 1–2 J/cm^2 at 1.06 μm, degradation in KTP is minimal for a pulse count up to 10^8–10^9. The KTP crystals are operated typically at 90°C. One investigation revealed that the dependence of the induced absorption of 532-nm radiation is nonlinear and has a threshold of 80 MW/cm^2 [11.52].

Experiments have also shown that the peak power threshold for gray-tracking damage strongly depends on the repetition rate of the laser. An exponential decrease of damage threshold as a function of repetition rate was observed, ranging from 125 MW/cm^2 at 1 kHz to 18 MW/cm^2 at 6.3 kHz, to a few MW/cm^2 for frequencies above 10 kHz [11.50].

Lithium niobate has a relatively low damage threshold in comparison with other common nonlinear materials. For example, at 1.06 μm, a surface damage threshold of 180 MW/cm^2 has been measured for a 10-ns pulse with a Gaussian intensity profile [11.54]. At a wavelength of 1.54 μm, a damage level of 20 J/cm^2 with a 50-ns long pulse has been reported [11.26].

$LiNbO_3$ is plagued by photorefractive effects resulting from propagation of visible or UV radiation. Photorefractive effects cause refractive index inhomogeneities which seriously degrade beam quality and distort the index-match condition necessary for efficient second-harmonic generation [11.55, 56]. The occurence of refractive index gradients is reversible if the temperature of the crystal is increased during operation to about 160°C. The index inhomogeneities are associated with imperfections in the crystal. Photons at the shorter wavelength have enough energy to break the binding energy which traps electrons at the vacant lattice site. The electrons are then free to move away, leaving behind a local electric field distribution in the crystal. Because of the large electro-optic effect of $LiNbO_3$, this local electric field causes refractive index gradients. Annealing the crystal at an elevated temperature increases the mobility of electrons in the crystal enough to permit neutralization of the charged vacancy, thereby removing the refractive index gradients. Also, doping with MgO has been used to reduce photorefractive damage; but doped crystals do not exhibit the same high quality that is available in undoped crystals.

There have been several reports that periodically poled lithium niobate is more resistant to photorefractive damage than are homogeneously poled crystals [11.57–59].

The large transparency range of 0.8–18 μm makes silver gallium selenide ($AgGaSe_2$) an excellent candidate for OPOs in the infrared region. Unfortunately, the crystal has a very low damage threshold which must be taken into account when engineering specific OPO devices. Measurements with a pump laser at 2.09 μm revealed an average surface damage threshold for coated and uncoated crystals of around 1 J/cm^2 at a pulse width of 50 ns [11.60].

Silver gallium sulfide ($AgGaS_2$) with a transmission range of 0.5–12 μm is another crystal for OPO devices in the mid- and far-infrared region. A surface damage threshold of 25–50 MW/cm^2 for 10-ns pulses at 1.064 μm has been measured [11.61]. Since the bulk damage threshold of this crystal is an order of magnitude higher, further improvements of the crystal might lead to a higher surface damage threshold.

11.3.5 Dielectric Thin Films

Multilayer dielectric films are generally the weakest elements of any laser system. Because of the relative complexity and variety of deposition factors, thin films vary greatly in purity, morphology, uniformity, and composition, depending, to a great extent, on the specifics of the fabrication process. In addition, residual stress, substrate cleanliness, and other extrinsic factors tend to reduce the thin-film damage level well below that expected for the same material in bulk form.

The usefulness of a dielectric coating for high-power applications depends on the choice of coating material, thin-film design, and deposition technique. Today's knowledge of coating failures distinguishes between homogeneous background absorption in the film and absorption at localized defects. Many investigations have shown that microscopic absorbing defects in the film are the initial sites of failure [11.62–65].

During evaporation, ejected particles of coating material from the source, or particles flaking from the chamber walls, can become embedded in the film and can initiate the growth of so-called nodular defects. Inclusions form a discontinuity in the coating stack disrupt the electric field distribution, resulting in localized electric field enhancement in the vicinity of the nodule. This leads eventually to significant heating of the localized region. The effects of laser conditioning are now commonly seen to be a result of the heating and subsequent ejection of such inclusions.

Numerous measurements have conclusively shown that the defect density and film roughness, caused by overcoated particles, are key indicators in determining the threshold of a dielectric coating [11.63, 64, 66]. In AR coatings, the field intensity is near maximum at the substrate surface, where the coating is most vulnerable owing to surface imperfection, embedded polishing materials, and poor film structure.

Therefore, the ultimate limit for AR coatings is the damage threshold of the uncoated substrate material. With HR coatings the substrate surface is shielded from the high field strength, and the ultimate limit of a perfect coating is determined by bulk values of the coating materials.

Thin films and multilayer stacks for optical components of solid-state lasers are usually produced by electron-beam (e-beam) evaporation.

The e-beam deposition process consists of an electron beam generated by thermionic emission from a filament. The beam is focused and directed by permanent magnets to a grounded source material. Advanced deposition techniques include the ion-assisted deposition technique and ion-beam sputtering. The former technique uses a conventional e-beam source to generate the deposition and an ion gun pointed at the optical substrate to increase the energy of the deposited particles. Ion beam sputtering uses an ion source that strikes a target to sputter atoms with high arrival energies onto the substrate. The higher energy of the deposited particles compared to e-beam deposition generates denser films with lower porosity.

Very large pieces of optics, such as employed in inertial confinement fusion drivers, are AR-coated by a sol-gel process [11.67]. Sol-gel coatings are very cost-effective methods to produce coatings on large optical substrates since these coatings can be applied in a dip or spin process at room temperature. The procedure involves the preparation of a solution of metal alkoxides which is converted by hydrolysis or heat to an oxide in a gelation stage. For example, from a solution of $Si(OCH_3)_4$ a SiO_2 coating can be produced. Very high damage thresholds can be achieved with sol-gel coatings. Drawbacks include their fragile nature and difficulty in cleaning the optical components. For this reason, sol-gel coatings are not often used in standard solid-state lasers. The AR coating of choice is usually vacuum-deposited MgF_2.

We will briefly review the laser-induced damage thresholds and major issues for thin-film coatings from the UV to the mid-infrared regime, which covers the range from frequency-quadrupled Nd:YAG lasers to OPOs operating in the 2–4 μm region.

The most detailed damage studies have been carried out for high-reflectivity HfO_2/SiO_2 coatings and for AR sol-gel coatings at the wavelengths of 1054 and 355 nm, because these coatings are used for the optical components of the large Nd:Glass lasers at the Lawrence Livermore National Laboratory.

UV Spectral Region. The damage threshold of dielectric thin films is lower in the UV region as compared to the longer wavelengths. One reason is the increased absorption, the other is the higher photon energy. Ionization and multiphoton absorption are more likely to occur at shorter wavelengths. The substrate materials transparent in the UV region are fused silica, MgF_2, and CaF_2. The choice of coating materials at the shortest wavelengths around 266 nm include MgF_2, LaF_3, SiO_2 and Al_2O_3. At the wavelength around 355 nm, ZrO_2 and HfO_2 can be added to the above-listed materials.

Table 11.2 lists laser-induced damage thresholds for common substrates and thin films employed in the UV region [11.68]. At 355 nm, the damage threshold of a HfO_2/SiO_2 high-reflectivity coating was measured between 5 and 8 J/cm^2 for a 3-ns

Table 11.2. Damage threshold [J/cm^2] at 248 nm of various substrates and coatings [11.68]

Substrate	
MgF_2 crystal	20
Quartz crystal	10
Suprasil 300	8
CaF_2	3
AR coatings	
MgF_2	9
LaF_3/MgF_2	10
Al_2O_3/SiO_2	3
Al_2O_3/MgF_2	3
HR coatings	
Al_2O_3/SiO_2	25
LaF_3/MgF_2	20

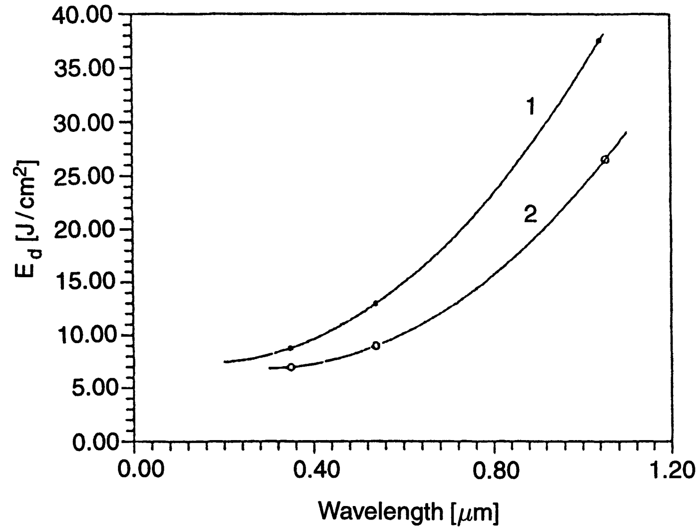

Fig. 11.7. Damage threshold of a multilayer ZrO_2/SiO_2 coating vs. wavelength for a defect density of $280/mm^2$ (*curve 1*) and $320/mm^2$ (*curve 2*) [11.69]

pulse. The damage threshold for ZrO_2/SiO_2 coatings was slightly lower, whereas Al_2O_3/SiO_2 coatings had damage thresholds around 10 J/cm^2 [11.66].

Visible and Near-Infrared Region. Multilayer thin films for this wavelength region usually consist of alternating layers of a metal oxide which provides the high-index material and SiO_2. Common combinations are HfO_2/SiO_2, ZrO_2/SiO_2, TiO_2/SiO_2, and Ta_2O_5/SiO_2. In particular, HfO_2/SiO_2 has a very high laser-induced damage threshold; it can be further improved with laser conditioning.

Damage threshold for a multilayer HfO_2/SiO_2 coating at 1.06 μm as a function of pulse width is depicted in Fig. 11.2. The damage threshold for a multilayer ZrO_2/SiO_2 coating measured versus wavelength with a 10-ns-long pulse and a Gaussian beam profile is shown in Fig. 11.7. The curves also illustrate the dependence of the damage threshold on defect density. Similar to the observation made with bulk materials (Fig. 11.5), there is a transition region with regard to the pulse width, where the damage morphology changes from heating and melting at the longer pulses, to ablation of the individual dielectric layers at very short pulses. At the short pulse-width regime, pulse-width scaling is less than $t_p^{0.5}$. Figure 11.8 depicts the dependence of the damage threshold on pulse width of very short pulses for two multilayer dielectric polarizers [11.21]. Damage thresholds for polarizer coatings are typically lower than those of similar mirror coatings. For example, for 3-ns pulses, HfO_2/SiO_2 thin-film polarizers have a damage threshold after laser conditioning of around 15–20 J/cm^2, which is half the value compared to mirror coatings.

In [11.70] damage thresholds were reported for monolayer and multilayer coatings produced by different commercial suppliers. The results of the tests performed with 25-ps and 8-ns pulses at 1064 nm are summarized in Table 11.3. The data illustrate the large spread in the damage threshold for coatings from different vendors.

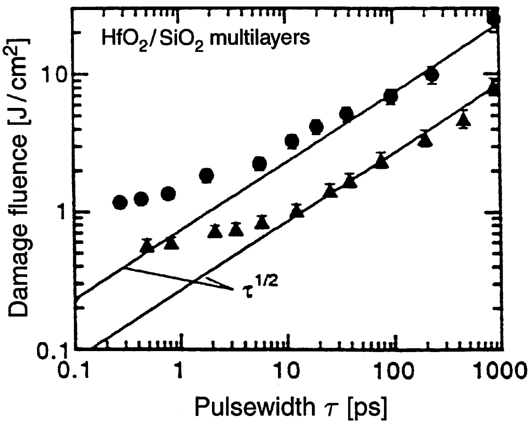

Fig. 11.8. Damage threshold at 1053 nm for HfO_2/SiO_2 multilayer 45° (▲) and 57° (●) polarizer [11.21]

The design and development of eye-safe rangefinders and LIDAR systems require high-damage-threshold coatings for the wavelength region around 1.5 μm. Measured values of the laser-induced damage threshold at this wavelength at a pulse width of 50 ns are listed in Table 11.4 for different coatings [11.26].

The damage threshold for ZrO_2/SiO_2 coatings were found to be higher as compared to TiO_2/SiO_2 (see also Fig. 11.4). The tests also revealed that the damage threshold for both types of coatings is about 20–30% higher at 1.5 μm as compared to 1.06 μm.

Mid-Infrared Spectral Range. Interest in high-power coatings for this wavelength regime is driven by the development of solid-state laser pumped OPOs with outputs between 2.5 and 4 μm. The availability of nonlinear crystals, such as KTA and PPLN, has opened the mid-infrared regime to solid-state lasers for a number of important applications such as atmospheric studies, spectroscopy, and IR countermeasures.

Table 11.3. Range of damage thresholds at 1064 nm (after preconditioning) for coatings produced by different commercial vendors [11.70]

	Damage threshold [J/cm^2]	
	25 ps	8 ns
Monolayers		
Ta_2O_5	4.6–5.4	25
TiO_2	3.1–3.4	9–18
SiO_2	15–16	140
Multilayer coatings		
ZrO_2/SiO_2	6.5–21.5	44–155
Al_2O_3/MgF_2	13–15	120–130
Substrate bare surfaces		
Fused silica	17.8–21.5	–
BK-7	20–21.5	–
Nd:YLF	10–12.5	–

Table 11.4. Damage threshold of multilayer coatings at 1.54 μm [11.26]

Materials and type of coatings	Number of layers	Laser-damage threshold at 1.54 μm [J/cm^2]
ZrO_2–SiO_2 high reflection	25	65 ÷ 80
ZrO_2–SiO_2 Partially reflective	10	No less than 100
TiO_2–SiO_2 high reflection	23	40 ÷ 60
ZrO_2–SiO_2 antireflection	2	No less than 100

Coatings have been well developed in this region as a result of DF and HF chemical laser systems. Dielectric thin films for optical parametric oscillators have special requirements, such as multi-wavelength and dichroic coatings.

Values for the laser damage threshold were reported in [11.71] for a number of dielectric thin films composed of different materials and deposited by different methods. The stacks were designed around the requirements for OPOs with reflection bands between 2.5 and 4 μm. The highest damage thresholds were found for the ZnS/Al_2O_3 films deposited by e-beam evaporation on either silicon, CaF_2, or ZnS substrates. Damage levels at 3.8 μm for a 55-ns pulse were around 50 J/cm^2, which is close to the damage level of the bare silicon substrate. Stacks of SiO_2/TiO_2 thin films also performed well with damage levels on the order of 45 J/cm^2.

11.4 System Design Considerations

The designer of a laser system, although he cannot change the damage thresholds of the materials employed in a laser, can reduce the damage susceptibility and improve the reliability of his system by the right choice of materials and by proper design and operation of the laser. We will enumerate a few design, inspection, and operating procedures which need to be followed to reduce the likelihood of optical damage to the laser components.

11.4.1 Choice of Materials

In powerful lasers it is important that only high-damage-resistance AR and multilayer coatings are employed. These coatings usually include ZrO_2, SiO_2, TiO_2, Al_2O_3, HfO_2, and MgF_2 compositions which are evaporated with an e-beam gun. Beam splitters, lenses, and prisms located in the beam have to be fabricated from fused silica, sapphire, or highly damage-resistant glass, such as BK-7. The surfaces of these components should be pitch-polished to a 5/10 or 0/0 surface quality. Surface conditioning or "superpolishing," such as chemical etching, ion-beam polishing, laser conditioning, or bowl-feed polishing, are very effective in raising the damage threshold.

All components of the laser system should be inspected for surface defects, such as scratches, fingerprints, "orange peel," and bulk defects, such as inclusions, bubbles, striation, schlieren, and internal stress.

Inclusions in a laser rod can be best checked by illuminating the rod from the side and observing the presence of scatter centers. The fringe pattern obtained from the Twyman-Green interferometer will reveal any density gradients and optical inhomogeneities in the laser rod. Inspection of the laser rod, Q-switch crystal, frequency doubling crystal, etc. between cross-polarizers will reveal internal stresses, striation, and schlieren. Optical surfaces are best inspected under a binocular microscope (magnification of 50×) with a strong collimated light beam reflected off the surface.

11.4.2 Design of System

One of the most, important considerations in the design of a laser system is the choice of beam size. This usually requires a trade-off between performance, which increases with higher fluence levels, and damage considerations which favor a larger beam size. Reliable operation requires that the beam diameter and, therefore, the aperture of all optical elements are large enough so that the power and energy densities are well below the damage threshold levels for the particular mode of operation.

The average power density of the beam is only an indicator, but not a reliable measure with regard to damage considerations. With Gaussian beams the peak intensity at the center rather than the average value has to be considered.

Hot spots in a multimode beam can far exceed average values; likewise, temporal fluctuations as a result of mode beating in multilongitudinal lasers can cause high-intensity temporal spikes.

As was discussed in Sect. 4.6 temporal spikes or disturbances in the spatial profile can lead to catastrophic self-focusing in high-power Q-switched lasers. A smooth temporal and spatial profile can be achieved with a laser operating in TEM_{00} mode and single line. To avoid self-focusing, high-power systems typically employ an injection-seeded oscillator lasing in a single transverse and longitudinal mode. Modulation of the beam profile by diffraction effects is reduced by employing spatial filters between amplifier stages.

The damage levels listed in this chapter have usually been measured in a carefully controlled laboratory environment, with smooth Gaussian beams, meticulously clean optics, and materials of excellent optical quality. The numbers clearly present upper limits. For a typical industrial or military laser employing industrial grade components and coatings the operating fluence and fluxes should be far below the numbers given for damage threshold.

A very important design consideration is the avoidance of damage caused by reflections from optical surfaces in the laser system. For example, very often a telescope is employed between amplifier stages to increase the beam diameter. The design and location of the negative lens employed in such a telescope is very critical, because if reflections from the concave surface are focused into the preceding laser rod, damage will most certainly occur. Therefore, a plano-concave rather than a concave–concave lens should be used and the curved surface should be faced away from the preceding optical components. In this case the reflected light from this surface is diverging rather than converging.

Reflections from the rear surface of an amplifier rod are very dangerous because the reflected radiation is amplified in passing through the amplifier stage, and optical elements at the input side of the amplifier, which are normally operated at much lower energy densities, can be damaged. This is especially the case if a telescope is employed between the oscillator and amplifier stage. If the beam travels backwards through the amplifier chain, the beam diameter decreases for increasing intensities, and damage thresholds are easily exceeded. One way to minimize this kind of damage is to tilt the various amplifier stages and separate them as far as possible from each other. A beam traveling backwards through an amplifier will then miss the aperture of the preceding stage. In order to suppress prelasing, which can cause the same type of damage, the amplifier rod should have wedged ends. Damage to optical surfaces can be minimized by employing highly damage-resistant coatings or by arranging the surfaces at Brewster's angle.

11.4.3 System Operation

Two common sources of damage are "hot spots" in the laser beam structure and contamination of optical surfaces. The peak fluence in a hot spot can exceed the average value by more than an order of magnitude. Damage sites caused by hot spots are usually much smaller than the beam area. Hot spots usually occur in multimode beams or they can be caused by diffraction effects. A small resonator misalignment brought about by vibration, or a change in the thermal conditions can lead to a change in mode structure with regions of high fluence.

Contamination of optical surfaces includes absorption sites such as dust or lint or debris from side lobes of the laser beam striking mirror mounts or other components, and absorption from fingerprints, water vapor, airborne oil from pumps, and outgassing from adhesives. Water vapor from a highly humid environment causing condensation leaves a residue after drying because it carries air pollutants, traces of tobacco smoke, sulfur compounds, etc.

Enclosing the beam path and filling the enclosure with a positive pressure of dry air usually eliminates the problem. From an operational point of view, the most important factors to consider, if damage is to be avoided, are proper alignment of components and absolute cleanliness of all surfaces. Misalignment of the oscillator components can cause a change of the transverse-mode structure, hot spots and beam uniformities can occur. Misaligned components outside the resonator cavity can cause undesirable secondary reflection leading to damage.

Surfaces which are contaminated by dust, dirt, or fingerprints will rapidly degrade and cause nonuniform beam intensities which, in turn, can cause damage in more expensive optical components. Surfaces should be inspected frequently and cleaned with an airblast or with alcohol. A dental mirror and a flashlight are very convenient for the inspection of optical surfaces in a laser system. Very often components are mounted close together and surfaces are hard to see. For the cleaning of surfaces which are relatively inaccessible, a stream of pressurized clean air or gas should be used. A useful device for cleaning optical surfaces is an ionizing airgun sold by 3M Company. The unit, which contains an α-particle source of polonium isotope 210 in the valve and nozzle sections, can be connected to a gas cylinder. The gas stream containing α-radiation can remove very efficiently statically charged particles from a surface.

The degradation and subsequent damage of optical surfaces by atmospheric dust particles and by cleaning residue has been studied by Barber [11.72]. It was found that dust particles consisting of minerals are melted onto the surface, leaving a circular indentation after the particle is dislodged by subsequent pulses.

In another type of degradation, craters are caused by liquids being absorbed a few micrometers into the glass surface during the cleaning operation, and then producing miniature explosions when a strong laser pulse strikes the absorbed liquid. Experiments showed that laser rod ends were badly pitted after liquid cleaning without drying, and no damage occurred on rods which were vacuum-dried.

From the foregoing it follows that the working area around a laser should be kept as clean as possible, free from dust and contaminants, such as cigarette smoke, so as to have clean room conditions as closely as possible.

After a laser is aligned and ready to be operated, the fluence level should be gradually increased starting at a level not higher than half the final output. This provides a chance for the removal of surface defects, and for particles to be evaporated or blown off by the shock wave created by the laser beam. Laser conditioning of coatings and bulk materials is an important procedure in achieving higher damage thresholds, as was discussed earlier in this chapter.

For lasers which are hermetically sealed, a few precautions are necessary to avoid contamination of optical surfaces by the environment created within the enclosure. It has been shown that trace levels of gas-phase contaminants of hermetically sealed Q-switched Nd:lasers can reduce the laser reliability and lifetime, especially for operation at elevated temperatures, i.e., above 50°C [11.73]. In these life tests, outgassing from silicone materials used in o-rings, potting materials, and thermally conductive pads were evaluated for their damage potential, along with trace levels of solvents used in cleaning mechanical and optical components.

All silicone materials, except a space-grade encapsulant (Dow Corning 93–500) were found to have a high probability of inducing contamination damage in sealed Nd:YAG lasers. With regard to the cleaning fluids, the aromatic hydrocarbons (benzene derivatives, i.e., toluene) more readily caused damage than nonaromatics, i.e., acetone. Additionally, the presence of oxygen was shown to dramatically inhibit contamination damage due to hydrocarbons. Therefore, purging a hermetically sealed laser with dry air rather than dry nitrogen can significantly reduce optical damage due to outgassing. Implementation of the test results increased the laser operation at 70°C from less than 20 h to over 500 h without significant optical damage.